Journal of Neurochemistry, 2007, **101**, 1338–1350 doi:10.1111/j.1471-4159.2006.04437.x

Formation of cellular projections in neural progenitor cells depends on SK3 channel activity

Stefan Liebau,* Bianca Vaida,* Christian Proepper,* Stephan Grissmer,† Alexander Storch,‡ Tobias M. Boeckers,* Paul Dietl§ and Oliver H. Wittekindt§

**Department of Anatomy and Cell Biology, University of Ulm, Ulm, Germany*

†*Department of Applied Physiology, University of Ulm, Ulm, Germany*

‡*Department of Neurology, Technical University of Dresden, Dresden, Germany*

§*Department of General Physiology, University of Ulm, Ulm, Germany*

Abstract

Ion channels are potent modulators for developmental processes in progenitor cells. In a screening approach for different ion channels in neural progenitor cells (NPCs) we observed a 1-ethyl-2-benzimidazolinone (1-EBIO) activated inward current, which could be blocked by scyllatoxin (ScTX, IC_{50} = 2 ± 0.3 nmol/L). This initial evidence for the expression of the small conductance Ca^{2+} activated K^+-channel SK3 was confirmed by the detection of SK3 transcripts and protein in NPCs. Interestingly, SK3 proteins were highly expressed in non-differentiated NPCs with a focused localization in lamellipodia as well as filopodial structures. The activation of SK3 channels using 1-EBIO lead to an immediate filopodial sprouting and the translocation of the protein into these novel filopodial protrusions. Both effects could be prevented by the pre-incubation of NPCs with ScTX. Our study gives first evidence that the formation and prolongation of filopodia in NPCs is, at least in part, effectively induced and regulated by SK3 channels.

Keywords: calcium-activated potassium channels, filopodia, neural progenitor cells, SK3 channel.

J. Neurochem. (2007) **101**, 1338–1350.

Expression, localization and specific activation of different ion-channels are known to be vital during development and maturation of undifferentiated stem and progenitor cells (Cai *et al.* 2004; Deisseroth *et al.* 2004). During these processes stem cell morphology is characterized by the dynamic formation and reorganization of small cell compartments like filopodia and lamellipodia. These cell protrusions serve the exploration of the local environment, interaction with other cells and cell migration. The structural basis for the development and shape of these compartments are cytoskeletal proteins that are organized as dynamic macromolecular complexes (Mejillano *et al.* 2004) and their modulation depends on ion channels (Espinosa *et al.* 2002; Lauritzen *et al.* 2005; Ngo-Anh *et al.* 2005). Especially Ca^{2+}-activated voltage independent K^+ channels (K_{Ca} channels) influence the reorganization of lamellipodia (Schwab *et al.* 1999; Espinosa *et al.* 2002) and dendritic spines (Ngo-Anh *et al.* 2005).

K_{Ca} channels form two subfamilies of potassium channels, intermediate conductance and small conductance K^+ channels (IK and SK). They are activated upon elevated intracellular Ca^{2+} (Fanger *et al.* 1999; Keen *et al.* 1999; Schumacher *et al.* 2001; Bruening-Wright *et al.* 2002). So far, Ca^{2+} is the only known activator of K_{Ca}-channels and once activated, they can be kept in an open conformation by 1-ethyl-2-benzimidazolinone (1-EBIO) and its derivatives (Devor *et al.* 1996; Pedersen *et al.* 1999; Pedarzani *et al.* 2001). But only SK-channels can be selectively blocked by Apamine and Scyllatoxin (Chicchi *et al.* 1988; Ishii *et al.* 1997; Jager and Grissmer 2004). This subfamily consists of three members, SK1 (K_{Ca}2.1), SK2 (K_{Ca}2.2) and SK3 (K_{Ca}2.3) (Kohler *et al.* 1996).

Received August 3, 2006; revised manuscript received December 7, 2006; accepted December 9, 2006.

Address correspondence and reprint requests to Dr. Oliver H. Wittekindt, Department of General Physiology, University of Ulm, Albert-Einstein-Allee 11, 89081 Ulm, Germany.

E-mail: oliver.wittekindt@uni-ulm.de

Abbreviations used: 1-EBIO, 1-ethyl-2-benzimidazolinone; NPC, neural progenitor cell; PBS, phosphate-buffered saline; PLL, poly-L-lysine; RT-PCR, reverse transcriptase-polymerase chain reaction.

In this study, we investigated the expression and biological function of K_{Ca}-channels in long-term cultured neural progenitor cells (NPCs), which are self-renewing progenitors and have the ability to differentiate into all cell types of the central nervous system (CNS). Up to now, however, the molecular mechanisms underlying the maturation and differentiation of NPCs are only poorly understood. In the light of the characterization of endogenous NPCs in the mammalian brain or *in vitro* cultured NPCs, possibly used for regenerative approaches in neurodegenerative conditions, the identification of factors that are essential for the structural reorganization of those cells is of special importance. We could demonstrate that SK3 channels are specifically expressed and localized in NPCs and we could show their impressive functional potency since the activation of these channels leads to a very rapid, enormous sprouting of filopodia in NPCs.

Materials and methods

Expansion of mesencephalic NPCs

Adult pregnant Sprague-Dawley rats were anesthetized and killed with 100% CO_2, embryos (embryonic stage E14.5) were removed from the uterus and placed into ice-cold Hank's balanced salt solution (HBSS) supplemented with 1% penicillin/streptomycin and 1% glucose (all from Gibco, Tulsa, OK, USA). Their brains were removed and the midbrain was then aseptically prepared. The meninges were carefully removed from the tissue after preparation of the midbrain area. For expansion of neurospheres, tissue samples were incubated in 0.1% trypsin (Sigma, St Louis, MA, USA) for 10 min at 20°C, incubated in DNase I (40 mg/mL; Sigma) for 10 min at 37°C, and homogenized to a quasi single cell suspension by gentle triturating. The cells were added to 25-cm^2 flasks (2×3 10^6 viable cells per flask) in serum-free medium containing 63% DMEM high glucose, 32% Ham's F12, 1% glutamate, 2% B27 supplement, 1% penicillin/streptomycin and 1% non-essential amino acids (all from Gibco), supplemented with 20 ng/mL of the mitogen EGF (Sigma). Cultures were placed in a humidified incubator at 37°C and 5% CO_2, 95% air (21% O_2). After 4–7 days, sphere formation was observed. The medium was changed once a week while growth factor was added twice a week. The neurospheres were expanded for additional 3 weeks (in total three to five passages) in suspension before adherent proliferation was initiated by plating the cells (about 20 000\,cells/well) with the same media, supplemented with 5% serum replacement (Gibco) onto poly-L-lysine (PLL)-coated glass cover slips in 24-well plates. All following studies were then performed 1–24 h after transferring of the cells to the well-plates.

Electrophysiological experiments

Neurospheres were transferred onto poly-L-lysine coated glass cover slips and were kept under culturing conditions for 1–4 h before electrophysiological investigation. The cover slips were placed into a perfusion chamber directly before measurement and were permanently superfused with normal solution (N-sol, in mmol/L: NaCl 160, KCl 4.5, $CaCl_2$ 2, $MgCl_2$ 1, HEPES 5, pH 7.4) or potassium solution (K-sol, in mmol/L: KCl 164.5, $CaCl_2$ 2, $MgCl_2$ 1, HEPES 5, pH 7.4). Only those cells were taken for electrophysiological investigations, which had started to migrate from the attached neurosphere. Pipettes were pulled in three stages with a tip resistance ranging between 1.5 and 2.5 MΩ when filled with pipette solution (K-Asp, in mmol/L: K-aspartate 135, K-EGTA 10, $MgCl_2$ 2.2, $CaCl_2$ 7.09, HEPES 10 pH 7.2 which corresponds to a $[Ca^{2+}]_{free}$ of 500 nmol/L). A HEKA EPC9 amplifier (HEKA elektronik, Lambrecht, Germany) was used with Pulse and PulseFit as data acquisition and analysis software. The membrane potential was preconditioned to −120 mV for 50 ms followed by a 400 ms voltage ramp from −120 to +60 mV. The membrane potential was clamped to −80 mV for 5 s between voltage ramps. 1-EBIO was added to K-sol at a final concentration of 1 mmol/L. The effect of scyllatoxin (ScTX) was tested by the application of scyllatoxin to K-sol containing 1 mmol/L 1-EBIO in increasing concentrations of 1, 3, 10 and 30 nmol/L. Whole cell currents were measured at −110 mV and relative currents were calculated according to I_{ScTX}/I_{EBIO} with I_{EBIO} as the maximal inward current measured in K-sol containing 1 mmol/L 1-EBIO and I_{ScTX} as currents measured in K-sol with 1 mmol/L 1-EBIO containing ScTX. Relative currents were blotted as means ± SEM ($n = 4$) against the ScTX concentration and concentration–response curves were calculated as best fit through the data points according to the Hill equation $I_{ScTX}/I_{EBIO} = 1/(1 + [ScTX]/IC_{50})$ using the software package IGOR pro (version 3.12, WavMetrics Inc., Lake Oswego, OR, USA). The calculated ± values obtained from the fit routine gives the uncertainties of the fit.

Semi-quantitative real-time one-step reverse transcriptase-polymerase chain reaction

Semi-quantitative real-time one-step reverse transcriptase-polymerase chain reaction (RT-PCR) was carried out using the LightCycler System (Roche, Mannheim, Germany), and amplification was monitored and analyzed by measuring the binding of the fluorescence dye SYBR Green I to double-stranded DNA. As much as 1 μL of total RNA was reversely transcribed and subsequently amplified using QuantiTect SYBR Green RT-PCR Master mix (Qiagen, Hilden, Germany) and 0.5 μmol/L of both sense and antisense primers. Tenfold dilutions of total RNA were used as external standards. Internal standards and samples were simultaneously amplified. After amplification, melting curves of the RT-PCR products were acquired to demonstrate product specificity. Results are expressed relative to the housekeeping gene hydroxymethylbilane synthase (HMBS). Primer sequences, lengths of the amplified products and melting analyses are summarized in Table 1.

Western blotting

Whole cell protein extracts were separated by standard SDS polyacryl amid electrophoresis using a polyacrylamid gel with 8% total monomer concentration and were electro-blotted by standard protocols onto nitrocellulose membranes. SK3 specific antibodies (Alomone labs, Jerusalem, Israel) were diluted 1 : 400 of the recommended stock solution. As a negative control, antibodies were pre-incubated with their antigen prior to blot hybridization. The ECL detection kit (Amersham Pharmacia, Freiburg, Germany) was used for immune detection according to the manufactures protocol.

Table 1 Primer sequences and melting curve analysis of semi quantitative real time RT-PCR experiments

Gene name	Primer sequence	Product length (bp)	Melting curve
SK1 (Kcnn1)	5′-GAAGAAGCCAGACCAAGCC-3′ 5′-GCGATGCTCTGTGCCTTG-3′	147	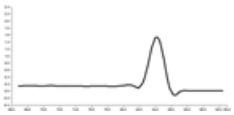
SK2 (Kcnn2)	5′-CTTTTCACCGATGCCTCCTC-3′ 5′-GCACAGTTCCTGGGCAGATAG-3′	106	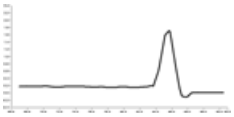
SK3 (Kcnn3)	5′-GAAAGCGACTGAGTGACTATGC-3′ 5′-GCAGGATGATGGTGGATAAAC-3′	153	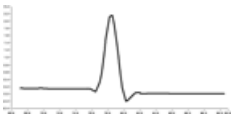
HMBS	5′-CGACACTGTGGTAGCGATGC-3′ 5′-CCTTGGTAAACAGGCTCTTCTCTC-3′	134	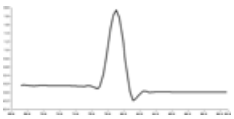

Names of gene products and gene names, primer sequences and product length are given. The melting curves are plotted as $dF(T)/dT$ (*y*-axis) against T [°C] (*x*-axis).

Immunocytochemical detection

For immunofluorescence detection, cultured cells were fixed with 4% paraformaldehyde (PFA)/1.5% sucrose/ phosphate-buffered saline (PBS) for 20 min at 20°C. After washing three times with 1X PBS for 5 min at 20°C the cells were permeabilized for 5 min on ice in a buffer containing 0.2% Triton-X-100/0.1% Na-Citrate/ PBS and washed again three times with 1X PBS. Blocking was performed with 10% FCS/PBS for 1 h at 20°C followed by incubation with the primary antibodies, diluted in PBS, for 3 h. After a further washing-step, the cells were incubated with the secondary antibody conjugates for 90 min at 20°C, washed three times with 1X PBS and then with aqua bidest for 3 min and mounted in Mowiol (Sigma). Cell nuclei were counter stained with 4,6-diamidino-2-phenylindole (DAPI). The following primary antibodies were used: rabbit anti-SK3 diluted 1 : 200, rabbit (Alomone Labs), mouse anti-Nestin monoclonal diluted 1 : 500 (BD Biosciences, Heidelberg, Germany), mouse anti-Fascin diluted 1 : 500, rabbit anti-VASP diluted 1 : 500 (both Millipore Billerica, MA, USA), mouse anti-ABI-1 diluted 1 : 250 (MBL Woburn, MA, USA), anti-IRSp53 diluted 1 : 1000 (Bockmann *et al.* 2002), anti-N-WASP diluted 1 : 500 (Santa Cruz, Santa Cruz, CA, USA); fluorescence labeled secondary antibodies were Alexa Fluor® 488 (green, used filter set: excitation BP 450–490, FT 510, emission BP 515–565 nm), Alexa Fluor® 568 (red, used filter set: excitation BP 534–558 nm, FT 560, emission BP 575–640 nm) and Alexa Fluor® 647 (magenta used filter set: excitation BP 610–670 nm, FT 660, emission BP 640–740 nm (Invitrogen, Karlsruhe, Germany) all diluted 1 : 500. Images were captured using an upright fluorescence microscope (Axioskop 2, Zeiss, Oberkochen, Germany) equipped with a Zeiss CCD camera (16 bits; 1280×1024 pixels per Image), and analyzed using Axiovision software (Zeiss).

Time lapse microscopy

Neurospheres were transferred to a two-well chamber slide coated with poly-L-lysine. Cells were allowed to attach to the coated glass surface and were kept under culturing conditions as described above for 2–24 h. The medium was exchanged against N-sol and the chamber slide was placed under a Richardson contrast microscope RTM-2.5 (Improvision, Tübingen, Germany) equipped with a water immersion objective (63X 0.92; Leica, Wetzlar, Germany) and a CCD camera (3CCD XwaveHAD; Sony, Berlin, Germany). Pictures were acquired every 4 s and analyzed using the velocity software package (Improvision). Compounds were added directly to the bath solution

Pre-embedding immunoelectron microscopy

Cells were fixed with 4% paraformaldehyde, 0.1% glutaraldehyde and 1% sucrose 10 min at 4°C and permeabilized through graded series of ethanol (10%, 15%, 20%, 15%, and 10% 10 min each at 20°C). Pre-incubation was carried out 30 min at 20°C with 10% normal goat serum, 1% BSA in PBS followed by incubation with the primary antibody rabbit anti-SK3 1 : 100 in 3% goat, 1% BSA in PBS overnight at 4°C. After washing a biotinylated goat anti-rabbit IgG antibody 1 : 100 was added for 2 h at 20°C (Vector, Burlingame, CA, USA). Cells were covered with a 1 : 100 dilution of the avidin–biotin–horseradish peroxidase complex (Vector) for 30 min. As substrate for the peroxidase 3,3-diaminobenzidine (DAB) was applied followed by a postfixation with 2.5% glutaraldehyde and 1% sucrose in 0.1 mol/L phosphate buffer pH 7.3. Cells were visualized for electron microscopy by silver staining, treated with 0.5% osmium tetroxide/0.8% $K_3Fe(CN)_6$ 20 min at 20°C, contrasted with 0.5% tannic acid and 2% uranylacetate and embedded in epoxy resin (FLUKA, Taufkirchen, Germany). Ultrathin sections (70–80 nm) were examined by using an EM10 transmission electron microscope at 80 kV (Zeiss).

Results

Electrophysiology

Whole cell currents were elicited using 200 ms voltage ramps from −120 to +60 mV. In N-sol outward ramp currents appeared at membrane potentials more positive than −20 mV. Inward currents measured at −110 mV were −11 ± 5 pA (mean ± SEM, $n = 7$). Exchanging N-sol against K-sol resulted in outward currents above 0 mV and inward currents below 0 mV. The inward currents measured at −110 mV were −84 ± 22 pA (mean ± SEM, $n = 7$), which were further increased to 235 ± 64 pA (mean ± SEM, $n = 7$) by 1 mmol/L 1-EBIO and blocked to 89% by 30 nmol/L ScTX (IC_{50} = 2 ± 0.3 nmol/L, Fig. 1).

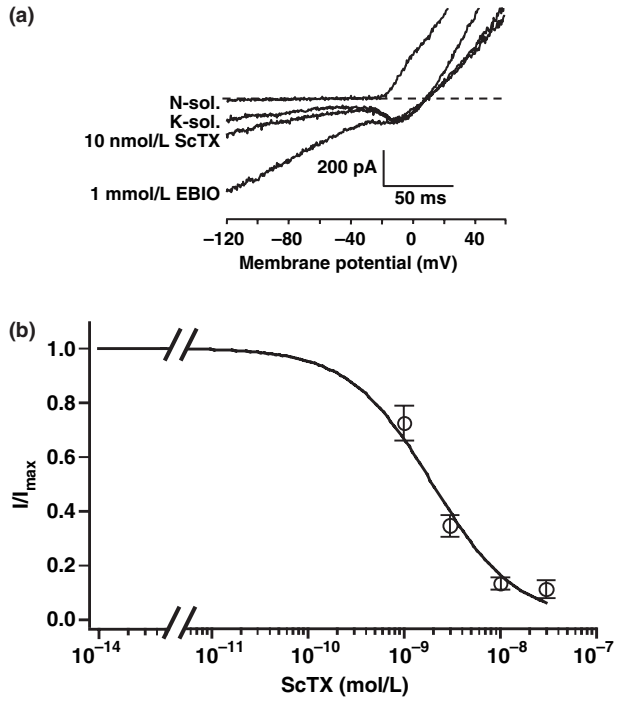

Fig. 1 Electrophysiological investigation of whole cell SK3 currents in neural progenitor cells. Cells were perfused with a K-Asp solution containing 500 nmol/L free Ca^{2+}. The membrane potential was ramped from −120 to +60 mV for 200 ms and was kept at −80 mV for 5 s between each voltage ramp. (a) Representative ramp currents are shown in normal solution (N-sol), potassium solution (K-sol), K-sol +1 mmol/L 1-ethyl-2-benzimidazolinone (1-EBIO) and K-sol +1 mmol/L 1-EBIO +10 nmol/L ScTX. The concentration response curve is given in (b). Relative currents were calculated as I/I_{max} with I as the currents with K-sol as bath solution containing 1 mmol/L 1-EBIO alone and together with 1, 3, 10 and 30 nmol/L ScTX and I_{max} as the maximum current measured in K-sol containing only 1 mmol/L 1-EBIO. The relative currents were plotted against the ScTX concentration as mean values ± SEM and the concentration response curve were calculated as best fit through the data points according to the Hill equation $I/I_{max} = 1/1 + ([ScTX]/IC_{50})$.

Semi-quantitative real-time one-step RT-PCR

Relative expression levels of SK channel transcripts were investigated by semi-quantitative RT-PCR (Fig. 2) on total RNA from cultured NPCs and rat whole brain (embryonic stage E20). The detected expression levels for NPCs were SK3 >>SK1 > SK2 (from highest to lowest). Interestingly, the expression levels of these transcripts in native tissues were SK1 >> SK3 > SK2 (from highest to lowest) and deviated therefore significantly from the levels observed in NPCs. Compared with previous studies the expression levels detected in our experiments for whole embryonic brain deviated from previous studies for human embryonic brain (Rimini *et al.* 2000). However, since both studies were carried out on different species and the developmental state of the tissues used by Rimini *et al.* (2000) was not closer defined, a direct comparison with our results is not possible.

Western blotting and Immunocytochemistry

SK3 protein was detected in Western blot experiments at an apparent molecular size of 50 kDa (Fig. 3a). Two additional bands at much lower signal intensities were detected at higher molecular weights. The pre-incubation of antibodies with the SK3 specific antigen suppressed the immune detection completely, assigning the detected signals as specific SK3 bands. The homogeneity of the progenitor population was proven by the positive staining of almost all cells by this antibody (Fig. 3b). Nestin-specific antibodies were used to identify undifferentiated NPCs. SK3 protein was detected in small clusters by SK3 specific antibodies in all nestin-positive cells. Within the cells, the SK3 staining was strongest in the distal parts of cell projections, the membrane and in a compartment juxtaposed to the nucleus. This staining can be interpreted as newly generated protein in the ER (Fig. 3c).

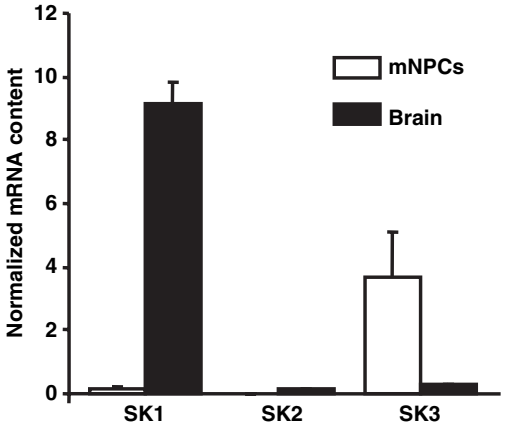

Fig. 2 Semi-quantitative real time RT-PCR from undifferentiated neural progenitor cells and embryonic whole brain at stage E20. Expression levels are shown relative to the housekeeping gene HMBS (Hydroxy-methyl bilane synthase, mean ± SEM, $n = 4$). Primers and melting curve analysis are given in Table 1.

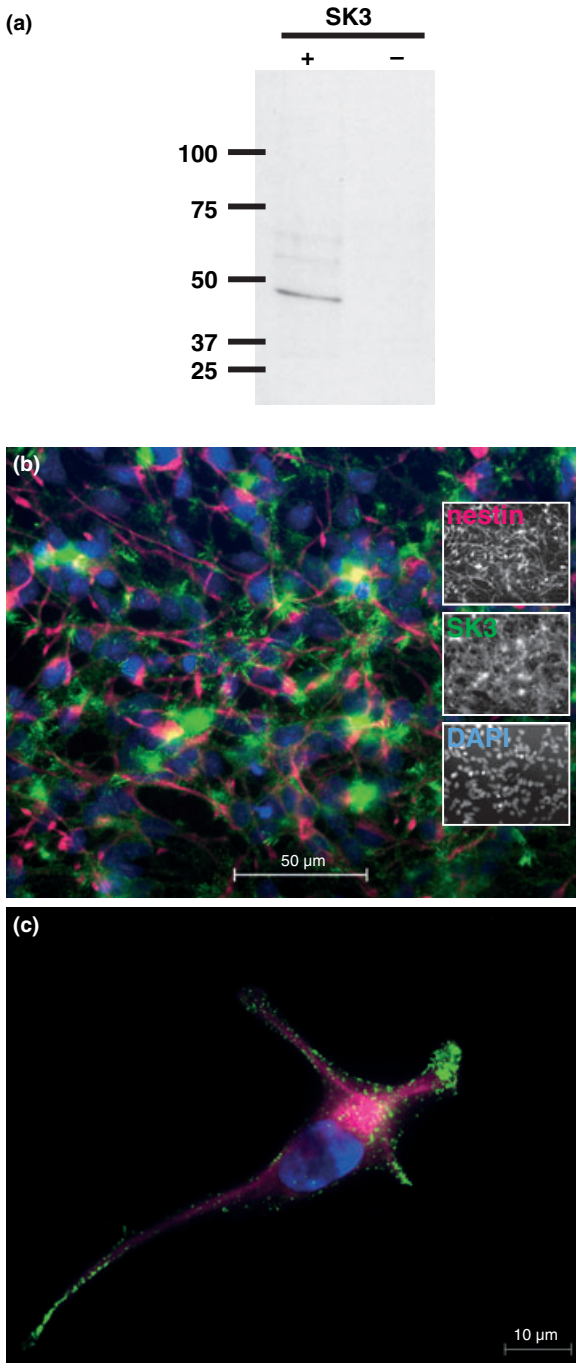

Fig. 3 Immuno detection of SK3 proteins in neural progenitor cells (NPCs). (a) Western blot of NPC whole cell protein extracts. A band at an apparent molecular weight of *ca.* 50 kDa was detected (lane marked with +). Antibody specificity was confirmed by pre-incubation of the antibody with its SK3 specific antigen (lane marked with –). (b) Immunocytochemical detection of SK3 subunits in undifferentiated NPCs. Nuclei were stained by DAPI (blue). Anti-nestin antibodies (magenta) were used to confirm the progenitor cell state. Almost all nestin-positive cells were found to be also positive for SK3 channels (green). (c) SK3 (green) is predominantly localized at the plasma membrane. (nestin = magenta; nucleus = DAPI; blue).

Time lapse microscopy

In order to investigate the possible role of these SK3 channels in NPCs, we performed time lapse experiments using the contrast mode of the Richardson Contrast Microscope. A continuous reorganization of filopodial and lamellipodial structures could be observed at the entire surface of NPCs in N-sol as extracellular solution. Under these conditions the outgrowth and retraction of short filopodia from existing filopodial buds as well as new formation of filopodia was observed. Application of the SK3-current potentiating substance 1-EBIO resulted in an overall flattening of the membrane surprisingly followed by a very fast sprouting of numerous new, extremely long filopodia within 5–10 min after 1-EBIO application. No retraction of the newly generated processes could be seen within the investigated time of up to 45 min (Fig. 4a–c, movie available as supplementary data online). The sprouting occurred in all membrane sectors and was not restricted to certain cellular regions. After the 1-EBIO induced cell protrusions reached their final length and no more sprouting could be observed, the adjacent application of the SK channel specific blocker ScTX (50 nmol/L), which inhibits K^+ currents mediated by SK3-channels state-independently did not lead to a retraction or any other effect on the newly generated filopodia. However, pre-incubation with ScTX for at least 10 mins before a successive application of 1-EBIO almost prevented growth of filopodial structures even after a time of 50 min in the presence of ScTX and 1-EBIO (Fig. 4d and e). This points to an ion-mediated mechanism. Thus ScTX was able to antagonize the 1-EBIO induced generation and protrusion of filopodia pointing out the specificity of the 1-EBIO-effect. Altogether, 15 cells from four independent isolations were investigated.

Phalloidin staining

Whether these formations were simple membrane protuberances or actin-based projections, the cytoskeleton protein β-actin was visualized by phalloidin staining. Under control conditions (Fig. 5a–c), the cells typically showed a slightly speckled staining pattern along their cellular body resembling the reported actin stars (Mejillano *et al.* 2004), projections with postulated parallel actin-formations called filopodia as well as actin-rich lamellipodia consisting of a meshwork of actin fibers with typical actin rims and ribs. The application of 1-EBIO (Fig. 5d–f) to the cell media resulted in the formation of actin-rich protrusions, which were distributed over the entire cell including elongation of microspikes. When ScTX solely was applied (Fig. 5g–i), the phalloidin staining of lamellipodia was more diffuse (shown in Fig. 5i) compared with the staining of control cells (shown in Fig. 5c), which is in good agreement with the loss of actin ribs. When 1-EBIO was added after NPCs were preincubated with ScTX, the phalloidin staining pattern was similar to control conditions (Fig. 5j–l).

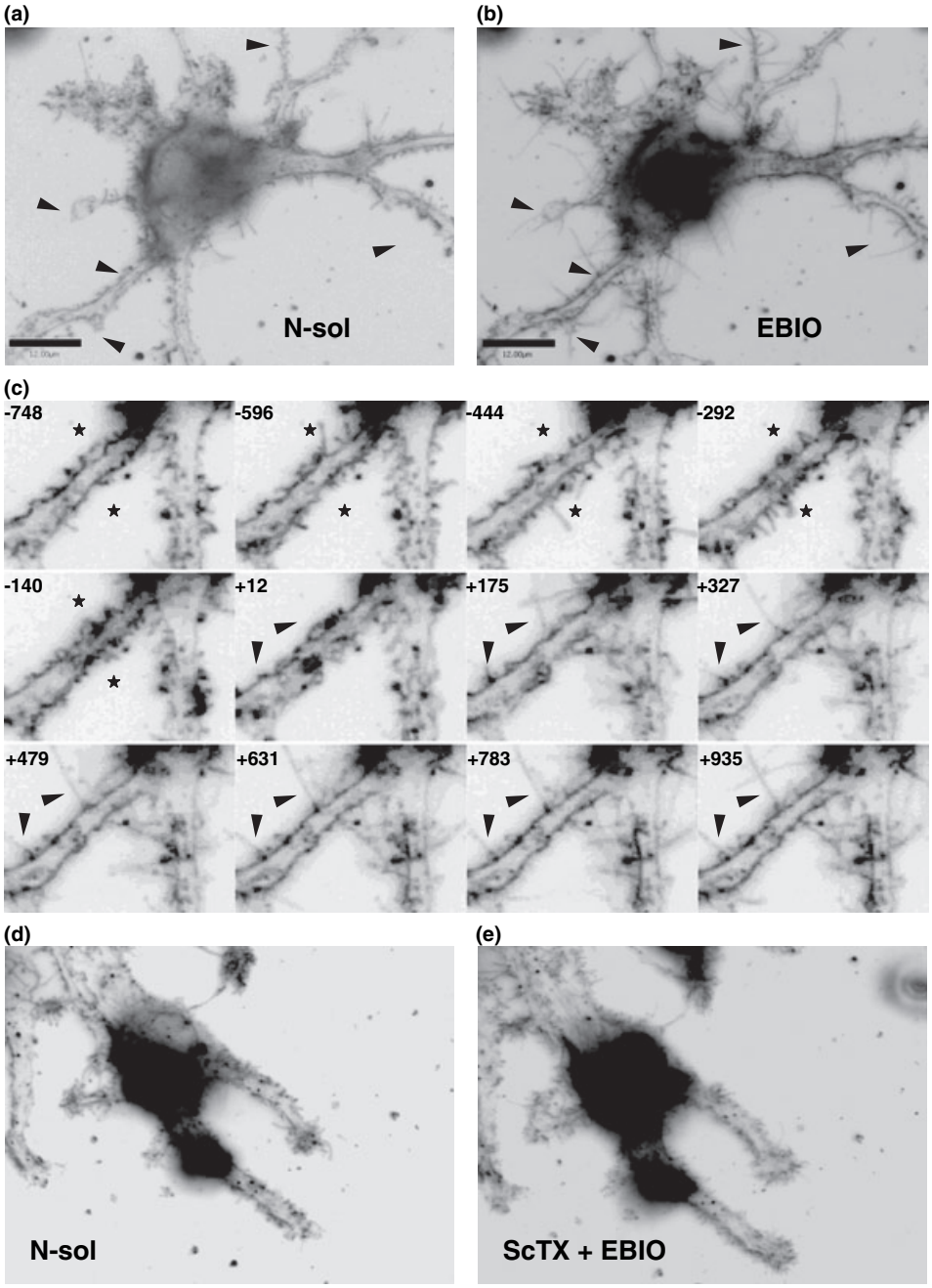

Fig. 4 Representative living neural progenitor cells (NPCs) shown in the contrast mode of the Richardson Contrast Microscope. (a) NPC under control condition with N-sol as extracellular solution (minutes 0–32) and (b) after 1-ethyl-2-benzimidazolinone (1-EBIO) application (minutes 32–52). Arrowheads point towards sites of 1-EBIO induced filopodial sprouting (First and last frame of time lapse experiment are shown). (c) Magnification of filopodial outgrowth over time. Numbers give seconds before (–) and after (+) 1-EBIO application. Stars label sites at which reversible filopodial sprouting occurs under control condition. Arrowheads points towards sites at which 1-EBIO induced filopodial outgrowth occurred. (d and e) Scyllatoxin prevented the 1-EBIO induced filopodial sprouting (First and last frame of frame of time lapse experiment are shown). (d) NPC under control conditions with N-sol as extracellular solution (minutes 0–11) and (e) after application of 50 nmol/L Scyllatoxin (minutes 11–23) and 1-EBIO (ScTX +1-EBIO, minutes 23–42).

We performed a statistical analysis of the total length of filopodia and number (Fig. 6a) of filopodia density (filopodia/μm of membrane perimeter, Fig. 6b). The filopodial length in untreated control cells ranged from 0.1 to 21.3 μm (1.5 ± 1.7 μm, mean ± SD; $n = 10$ cells, 588 filopodia). Cells treated with 1-EBIO alone showed significantly

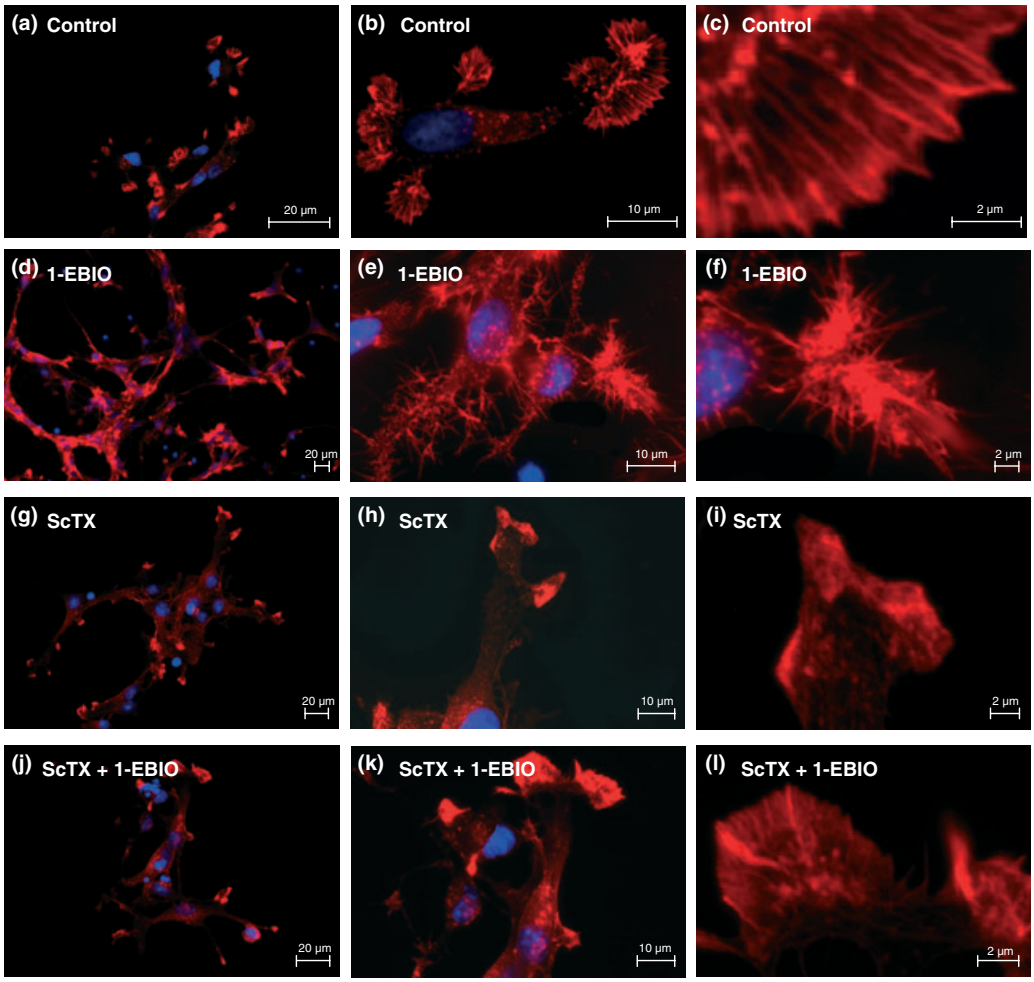

Fig. 5 Phalloidin staining of neural progenitor cells (blue = nuclei, DAPI and red = phalloidin, actin). Cells kept under control conditions are shown in (a–c). 1-Ethyl-2-benzimidazolinone induced the protrusion of strongly phalloidin positive actin rich protrusions, shown in (d–f). Scyllatoxin (ScTX) resulted in a morphological change of lamellipodia like structures shown in (g–i). ScTX also prevented the formation of phalloidin positive protrusions, when added before 1-EBIO application (j–l).

increased length of filopodia, ranging from 0.2 to 42 µm (6 ± 6 µm, mean ± SD; $n = 9$ cells, 907 filopodia). ScTX treatment resulted in a significant decrease in filopodial length ranging from 0.1 to 9 µm (1.2 ± 0.8 µm, mean ± SD; $n = 10$ cells, 272 filopodia). No significant difference vs. control cells could be observed in cells treated with ScTX +1-EBIO. Filopodial length ranged from 0.1 to 7.0 µm (1.7 ± 1.2 µm, mean ± SD; $n = 5$ cells, 146 filopodia). Also the filopodial density was found to be significantly increased in 1-EBIO treated NPCs compared with control conditions (EBIO treated cells 0.44 ± 0.13 filopodia/µm, control cells 0.22 ± 0.08 filopodia/µm, mean ± SD). Contrary to that the application of ScTX led to a significant decrease of filopodial length and density (0.11 ± 0.05 filopodia/µm). No significant difference was observed comparing control conditions with treatment of both ScTX plus 1-EBIO (0.2 ± 0.07 filopodia/µm). We also saw elongation of lamellipodia-embedded actin bundles (microspikes) independently from newly generated filopodia along the cell body.

The co-staining of the actin cytoskeleton and SK3 protein (Fig. 7) revealed that SK3 protein was localized in the 1-EBIO-induced phalloidin-positive protrusions (Fig. 7b and c).

Pre-embedding immunoelectron microscopy

Electron microscopic pictures showed intact protrusions of NPCs with an apparent width of 100–150 nm (Fig. 8). Silver particles, mainly associated with the membrane, are especially localized from the base up to the tip of these filopodial structures, indicating the localization of SK3 proteins to these regions.

Characterization of filopodia

The actin-rich cellular protrusions induced by 1-EBIO were identified as filopodia by positive immunostaining for

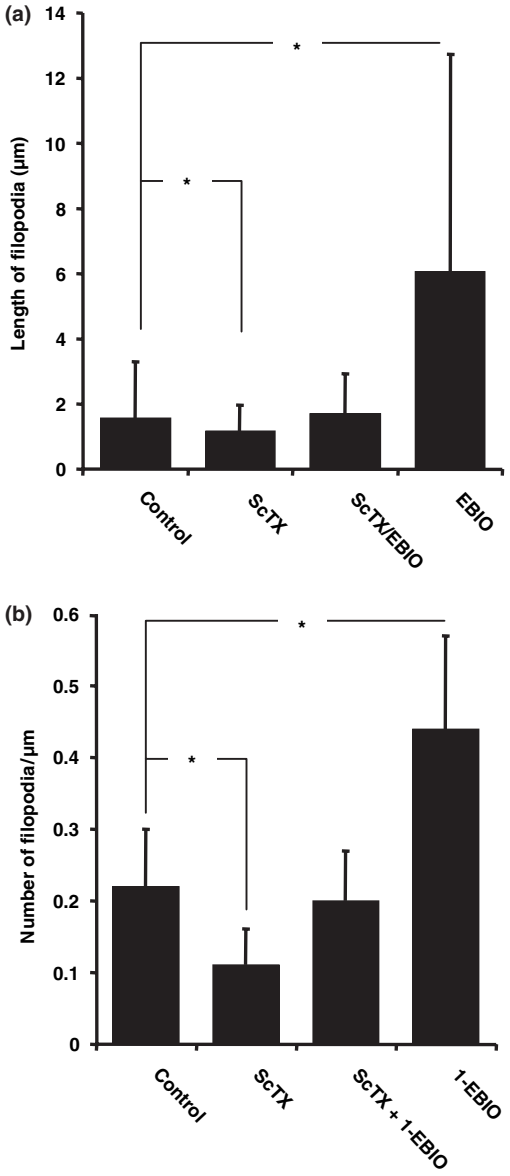

Fig. 6 Analysis of cellular protrusions in control and treated neural progenitor cells (NPCs). Control cells (control) and treated cells with ScTX, 1-ethyl-2-benzimidazolinone (1-EBIO) and ScTX +1-EBIO (ScTX/EBIO) were compared. Statistically significant differences (two tailed students *t*-test, $p < 0.05$) of NPC populations compared with control cells are marked with '*'. (a) The length of filopodia was significantly increased in 1-EBIO treated cells. ScTX treatment resulted in a significant decrease in filopodial length. No significant changes could be observed in NPCs treated with 1-EBIO together with ScTX (b). (a) The density of filopodia was significantly increased in 1-EBIO (EBIO) treated cells. ScTX treatment resulted in a significant decrease in filopodial density. No significant changes could be observed in NPCs treated with 1-EBIO together with ScTX.

known proteins being abundant in filopodia (Fig. 9). Fascin, a protein implicated to stabilize actin bundles in filopodia was observed along the actin-rich structures. Other proteins which drive filopodial formation like IRSp53 and ABI-1 (elongation of actin in the SOS-1/EPS8-complex (Stradal *et al.* 2001), or proteins which initiate the formation of filopodia like N-WASP (activator of the arp2/3 complex) and Ena/VASP family proteins (implicated in initiation and elongation) were detected in the proposed filopodia. SK3-proteins localized in the same structures. These findings give evidence that these 1-EBIO induced actin-rich structures were filopodia. Interestingly, SK3-protein showed a strongly overlapping localization with N-WASP, which is proposed to be part of the filopodial initiation complex.

Discussion

In the presented study, we sought to characterize NPCs with respect to their electrophysiological properties. We identified the SK3 channel to be responsible for the presence of an inward current in NPCs which was potentiated by the SK/IK specific activator 1-EBIO (Pedarzani *et al.* 2001) and could be blocked by ScTX.

The channels sensitivity to ScTX is clearly pointing towards the known properties of homomeric SK3 channels as already shown by heterologous expression of SK3 channels (Wittekindt *et al.* 2004). However, the heteromerization of SK channels is not completely understood and the expression and efficacy of heteromeric SK3 channels in NPCs may not be fully excluded based solely on the electrophysiological experiments. Considering the observation that SK3 channel transcripts were expressed at much higher levels in NPCs than SK2 or SK1 channel transcripts it is most likely that the detected 1-EBIO activated and ScTX sensitive whole cell inward currents in NPCs were carried by homomeric SK3 channels. There is strong evidence that the morphological changes which are directly linked to cellular differentiation events such as the formation of cellular projections and intercellular connections, are amongst others under control of Ca^{2+}-dependent second messenger systems (Cheng *et al.* 2002; Fink *et al.* 2003; Portera-Cailliau *et al.* 2003; Wayman *et al.* 2004; Lohmann *et al.* 2005). SK3 channels can be activated via an increase in intracellular Ca^{2+} concentrations and we demonstrated that the modulation of those channels by adding 1 mmol/L 1-EBIO to the extracellular solution resulted, compared with untreated controls, in an immediate sprouting of long, actin-positive filopodia. The pre-incubation of NPCs with ScTX almost prevented filopodial formation and elongation in the presence of 1-EBIO. The ability of ScTX to prevent filopodial growth showed that the observed effect is closely associated with SK3 channel activity. ScTX is known to block SK3 channels independently from its conformational state by binding to their outer pore region without inducing conformational changes. 1-EBIO is reported to keep activated SK3 channels in an open conformational state by interacting with the intracellu-

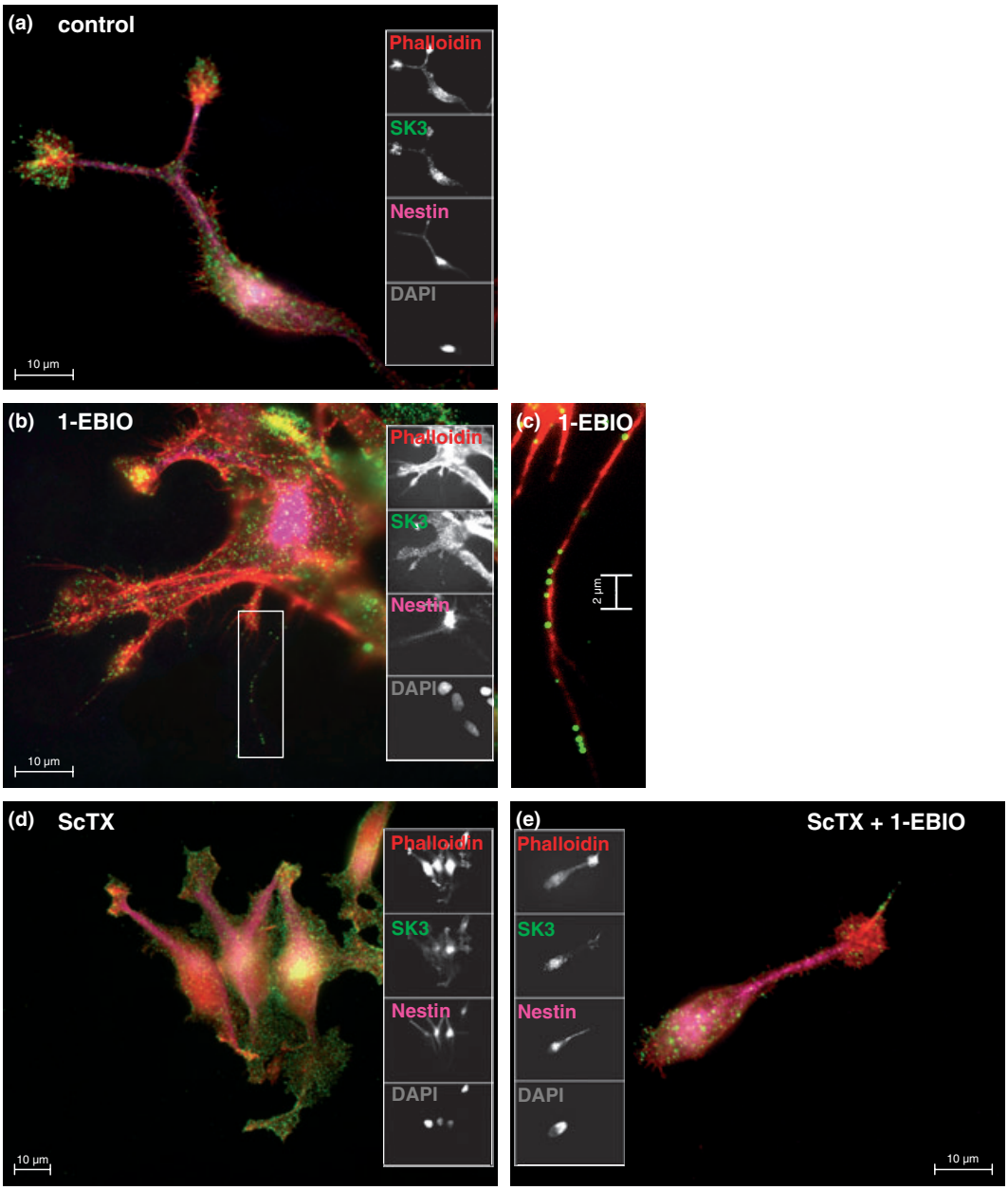

Fig. 7 Immunocytochemical detection of SK3 proteins [SK3 = green, Phalloidin (actin) = red, nestin = magenta, nuclei (DAPI) = only inset]. (a) Representative neural progenitor cell kept under control conditions. (b) Neural progenitor cell formed actin rich protrusions after 1-ethyl-2-benzimidazolinone application. (c) SK3 channels localized to 1-ethyl-2-benzimidazolinone induced filopodia. Representative cells in the presence of ScTX (d), and ScTX +1-EBIO (e).

lar C-terminal domain of the channel subunits. Both compounds bind reversibly to SK3 channels and do not compete with each other. The immunocytochemical investigation of SK3 expression revealed that almost all nestin-positive cells were also positive for SK3 protein. This observation confirmed once more the predominant SK3 expression in nestin-positive neural progenitor cells (NPCs).

Neural progenitor cells are known to be able to generate all cell types of the CNS. There is little known about the physiological reason and initiation signals for filopodial formation. NPCs and other stem or progenitor cells require a multitude of signals on their way from activation until integration into a functional tissue. Formation of cellular protrusions known to be necessary to investigate the surrounding, migrate along structures, hold tight to other cells and integrate into a cell network must therefore undergo a permanent specific reorganization of filopodial structures.

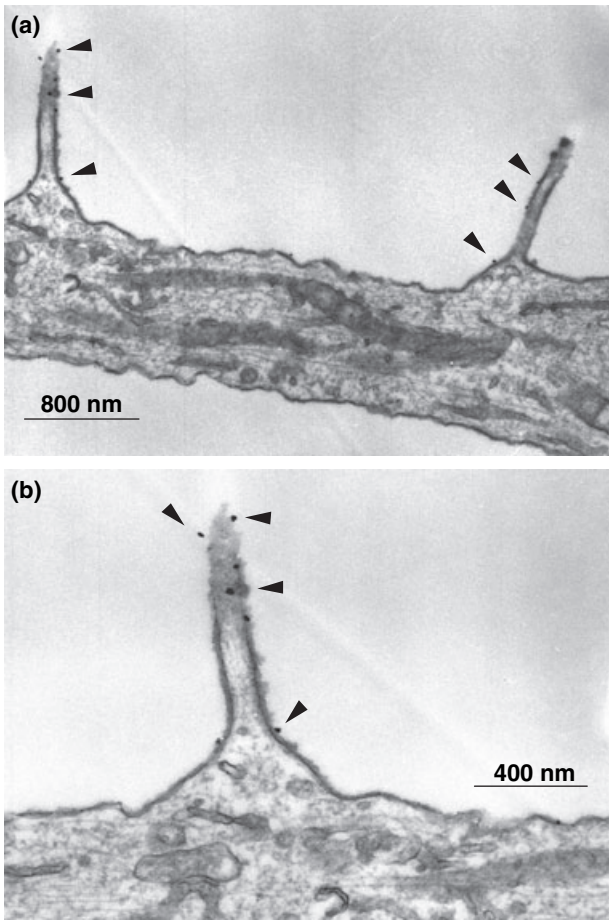

Fig. 8 Pre-embedding immunoelectron microscopy. Arrowheads point towards silver particles within cellular protrusions, which are immunopositive for the SK3 channel subunit. (a) Overview of cellular projection. (b) Detailed view of a single filopodial protrusion.

A variety of proteins and protein complexes have been described to induce and/or modulate the formation and elongation of filopodia. The filopodial machinery consists of proteins that initiate formation (a filopodia tip complex, FTP, is assembled, presumably at or very close to the plasma membrane). In addition, the FTP may contain proteins required both for actin filament nucleation and for reorganization of pre-existing filaments. In neuronal cells, e.g. N-WASP (Carlier *et al.* 1999; Yoo *et al.* 2006), formins, agrin (McCroskery *et al.* 2006), syndecan1 and WIP (Martinez-Quiles *et al.* 2001) are reported to initiate filopodial sprouting. Still, filopodial formation can be driven or modulated by different sets of proteins depending on cell type and organism. Proteins that uphold or drive filopodia elongation are amongst others the ABI-1 (Stradal *et al.* 2001), Arp2/3 complex, VASP or IRSp53 (Faix and Rottner 2006). Termination or blocking of filopodia elongation is mediated by the so called capping proteins and other actin depolymerization factors like cofilin (Fass *et al.* 2004). Small GTPases like Cdc42 (Hall and Nobes 2000) are known to be downstream molecules in the actin reorganization. Lamellipodia on the other hand have a different function for the cells, consist of a different meshwork of actin filaments and their architecture seems to be regulated by other proteins. In the lamellipodia in NPCs, we observed parallel bundled actin-formations called actin ribs or microspikes (Small *et al.* 2002). These formations are embedded in the meshwork of the lamellipodia and are thought to be able to develop into filopodia (Svitkina *et al.* 2003). These filopodial precursors were also found to protrude after 1-EBIO stimulation. Another important factor for the modulation of filopodia is the transport machinery into these structures. Myosins (X/VII) were reported to be responsible for the specific transport of proteins to filopodial structures (Tokuo and Ikebe 2004; Zhang *et al.* 2004; Sousa and Cheney 2005; Bohil *et al.* 2006).

It has been shown that intracellular ion concentrations are involved in modulating the reorganization of the actin cytoskeleton by at least two pathways. On the one hand the assembly of actin monomers can be affected by changes of intracellular potassium concentrations (Carlier 1991; Guan *et al.* 2005; Ouyang *et al.* 2005). On the other hand, it may influence proteins, which are involved in the reorganization of the actin cytoskeleton (Cao *et al.* 2006; Jung *et al.* 2006). The second hypothesis could be supported by the observation that SK3 channels showed an overlapping localization with N-WASP, a member of the filopodial initiation complex (Carlier *et al.* 1999; Yoo *et al.* 2006). However, it has been recently described that filopodia formation, at least in mammals, can occur in absence of WASP/WAVE family proteins. Though N-WASP was reported to be crucial for the Cdc42-induced filopodia formation, generation and elongation of filopodia also occurs in N-WASP deficient cells, suggesting other pathways besides, which remain elusive up to now (Snapper *et al.* 2001; Steffen *et al.* 2006).

The used SK3 channel modulators 1-EBIO and ScTX are known to interact directly with the functional channel and do not alter any channel protein interactions. Therefore, we hypothesize that local changes of K^+-homoeostasis specifically regulates or modulates the driving force for filopodia initiation and/or elongation. Our observation that treatment of the cells with ScTX adjacent to 1-EBIO exposure did not reduce the number of filopodia can be explained by our suggested mechanism that filopodial growth is initiated by local ionic changes taking influence on the initiation machinery of filopodia. Our observations suggest that it is more likely that there is a certain influence on the initiation machinery rather than on filopodial retraction.

The influence of K_{Ca} channels on distinct cellular compartments has already been shown for osteoclasts where they modulate membrane spreading (Espinosa *et al.* 2002). It was recently reported that different types of K^+ channels,

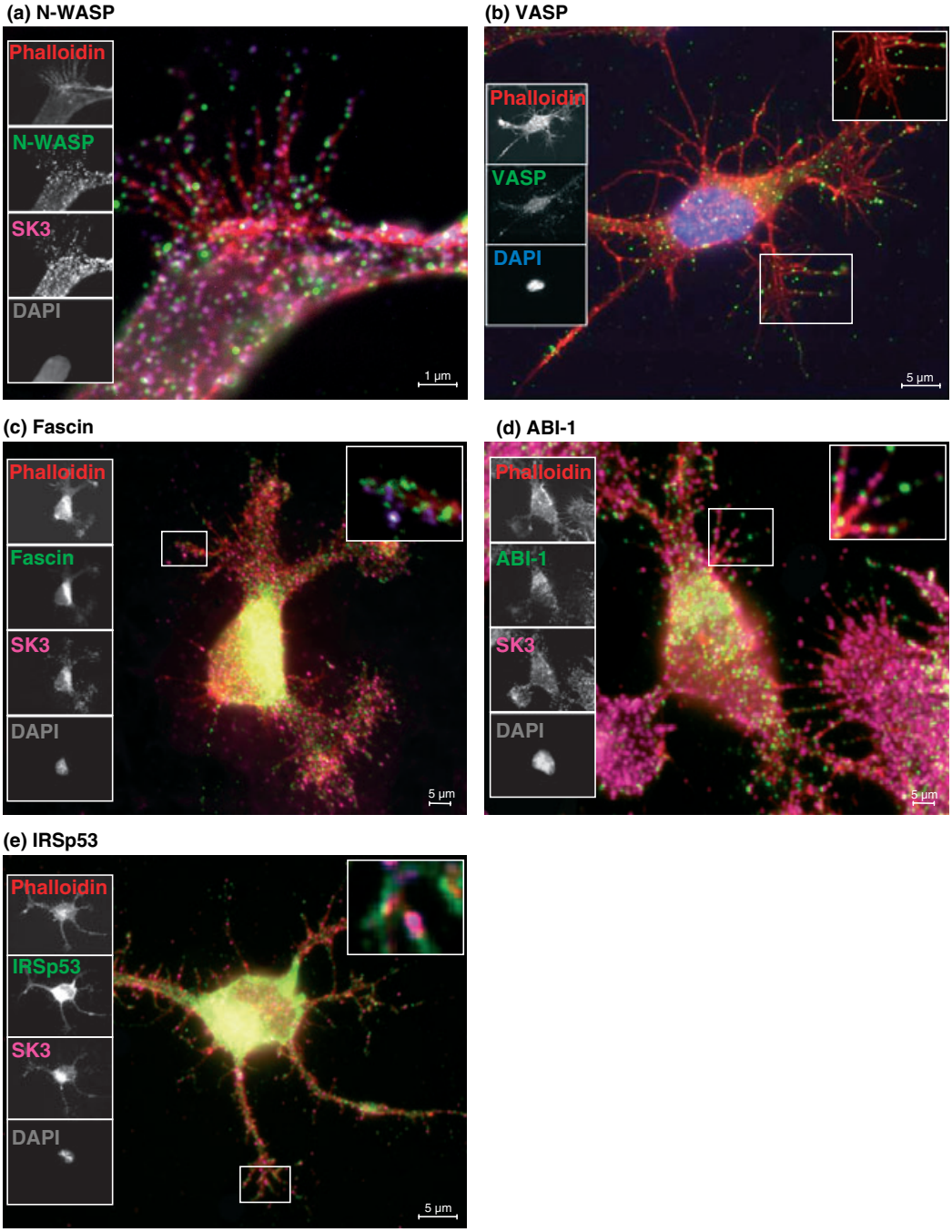

Fig. 9 Immunocytochemical detection of filopodial proteins in neural progenitor cells after 1-ethyl-2-benzimidazolinone stimulation [N-WASP (a); VASP (b); Fascin (c); ABI-1 (d); IRSp53 (e) = green, Phalloidin (actin) = red, SK3 = magenta, nuclei (DAPI) = only inset]. SK3 channels localized to 1-ethyl-2-benzimidazolinone induced filopodia.

like $K_v4.2$ (Petrecca *et al.* 2000), SK2 (Ngo-Anh *et al.* 2005) and TREK1 (Lauritzen *et al.* 2005), are located within filopodia-like structures. These channels were shown to interact directly or via scaffold proteins with the actin cytoskeleton. The observed modulating effect of SK3 channels on the reorganization of the actin cytoskeleton is more likely independent from any direct protein–protein interaction since both, ScTX and 1-EBIO, are known to affect the K^+ currents through SK3 channels and not the channel's conformation. Concerning the filopodial modulation our experiments give evidence that a direct conformational interaction between the channel and the cytoskeleton can be excluded as a major mechanistical component of the 1-EBIO induced reorganization of the

cytoskeleton. We therefore favor a model, in which the 1-EBIO induced activation of the voltage independent and non-rectifying SK3 channels leads to a K^+ efflux and results in a decreased intracellular K^+ concentration. This would be in good agreement with the observation that actin monomers form extended actin filaments in the absence of K^+ or at low K^+ concentrations. The formation and modulation of cellular extensions and rim structures are important mechanisms in many different cellular processes like the formation of intercellular contacts, path finding, migration and exploring the extracellular environment (Jacinto and Wolpert 2001; Rorth 2003). Those extensions are discussed to be formed randomly and being stabilized upon an appropriate stimulus (Rorth 2003). We showed that the activation of SK3 channels induces a non-reversible formation and protrusion of filopodia in NPCs. A possible role of SK3 channels might therefore be that environmental changes trigger SK3 channel activity (+ or −) which leads to a reorganization of filopodial protrusions, possibly to adjust intercellular contacts with following integrational processes or to modulate the cell migration. Questions remain about the molecular effect on the actin-machinery concerning SK3-activity. The physiological role of the highly-expressed SK3-channels combined with obvious filopodial modulation underlines the importance of this protein for NPCs.

Acknowledgment

We thank Eberhard Schmid and Paul Walther from the Central Electron Microscopy Unit. This work was supported by Grants: Wilhelm Sander-Stiftung (2004.046-1 to SG), 4SC (Martinsried Germany to SG), Medizinische Fakultät (University of Ulm, P770 to OW and P868 to SL), FWF (P15742 and P15743 to PD) and by the Land Baden-Württemberg (1423/74 to StL, TMB and SG).

References

Bockmann J., Kreutz M. R., Gundelfinger E. D. and Bockers T. M. (2002) ProSAP/Shank postsynaptic density proteins interact with insulin receptor tyrosine kinase substrate IRSp53. *J. Neurochem.* **83**, 1013–1017.

Bohil A. B., Robertson B. W. and Cheney R. E. (2006) Myosin-X is a molecular motor that functions in filopodia formation. *Proc. Natl Acad. Sci. U. S. A.* **103**, 12 411–12 416.

Bruening-Wright A., Schumacher M. A., Adelman J. P. and Maylie J. (2002) Localization of the activation gate for small conductance Ca2+-activated K^+ channels. *J. Neurosci.* **22**, 6499–6506.

Cai J., Cheng A., Luo Y., Lu C., Mattson M. P., Rao M. S. and Furukawa K. (2004) Membrane properties of rat embryonic multipotent neural stem cells. *J. Neurochem.* **88**, 212–226.

Cao W., Goodarzi J. P. and De La Cruz E. M. (2006) Energetics and kinetics of cooperative cofilin-actin filament interactions. *J. Mol. Biol.* **361**, 257–267.

Carlier M. F. (1991) Actin: protein structure and filament dynamics. *J. Biol. Chem.* **266**, 1–4.

Carlier M. F., Ducruix A. and Pantaloni D. (1999) Signalling to actin: the Cdc42-N-WASP-Arp2/3 connection. *Chem. Biol.* **6**, R235–240.

Cheng S., Geddis M. S. and Rehder V. (2002) Local calcium changes regulate the length of growth cone filopodia. *J. Neurobiol.* **50**, 263–275.

Chicchi G. G., Gimenez-Gallego G., Ber E., Garcia M. L., Winquist R. and Cascieri M. A. (1988) Purification and characterization of a unique, potent inhibitor of apamin binding from Leiurus quinquestriatus hebraeus venom. *J. Biol. Chem.* **263**, 10 192–10 197.

Deisseroth K., Singla S., Toda H., Monje M., Palmer T. D. and Malenka R. C. (2004) Excitation-neurogenesis coupling in adult neural stem/progenitor cells. *Neuron* **42**, 535–552.

Devor D. C., Singh A. K., Frizzell R. A. and Bridges R. J. (1996) Modulation of Cl- secretion by benzimidazolones. I. Direct activation of a Ca(2+)-dependent K+ channel. *Am. J. Physiol.* **271**, L775–784.

Espinosa L., Paret L., Ojeda C., Tourneur Y., Delmas P. D. and Chenu C. (2002) Osteoclast spreading kinetics are correlated with an oscillatory activation of a calcium-dependent potassium current. *J. Cell Sci.* **115**, 3837–3848.

Faix J. and Rottner K. (2006) The making of filopodia. *Curr. Opin. Cell Biol.* **18**, 18–25.

Fanger C. M., Ghanshani S., Logsdon N. J., Rauer H., Kalman K., Zhou J., Beckingham K., Chandy K. G., Cahalan M. D. and Aiyar J. (1999) Calmodulin mediates calcium-dependent activation of the intermediate conductance KCa channel, IKCa1. *J. Biol. Chem.* **274**, 5746–5754.

Fass J., Gehler S., Sarmiere P., Letourneau P. and Bamburg J. R. (2004) Regulating filopodial dynamics through actin-depolymerizing factor/cofilin. *Anat. Sci. Int.* **79**, 173–183.

Fink C. C., Bayer K. U., Myers J. W., Ferrell J. E. Jr, Schulman H. and Meyer T. (2003) Selective regulation of neurite extension and synapse formation by the beta but not the alpha isoform of CaMKII. *Neuron* **39**, 283–297.

Guan J. Q., Takamoto K., Almo S. C., Reisler E. and Chance M. R. (2005) Structure and dynamics of the actin filament. *Biochemistry* **44**, 3166–3175.

Hall A. and Nobes C. D. (2000) Rho GTPases: molecular switches that control the organization and dynamics of the actin cytoskeleton. *Philos. Trans. R. Soc. Lond. B Biol. Sci.* **355**, 965–970.

Ishii T. M., Silvia C., Hirschberg B., Bond C. T., Adelman J. P. and Maylie J. (1997) A human intermediate conductance calcium-activated potassium channel. *Proc. Natl Acad. Sci. U. S. A.* **94**, 11 651–11 656.

Jacinto A. and Wolpert L. (2001) Filopodia. *Curr. Biol.* **11**, R634.

Jager H. and Grissmer S. (2004) Characterization of the outer pore region of the apamin-sensitive Ca^{2+}-activated K^+ channel rSK2. *Toxicon* **43**, 951–960.

Jung J., Park H., Kim M., Kim M. J., Choi E. C. and Lee K. (2006) Extracellular potassium deprivation reversibly dephosphorylates cofilin. *Biochem. Biophys. Res. Commun.* **345**, 1393–1397.

Keen J. E., Khawaled R., Farrens D. L., Neelands T., Rivard A., Bond C. T., Janowsky A., Fakler B., Adelman J. P. and Maylie J. (1999) Domains responsible for constitutive and Ca(2+)-dependent interactions between calmodulin and small conductance Ca(2+)-activated potassium channels. *J. Neurosci.* **19**, 8830–8838.

Kohler M., Hirschberg B., Bond C. T., Kinzie J. M., Marrion N. V., Maylie J. and Adelman J. P. (1996) Small-conductance, calcium-activated potassium channels from mammalian brain. *Science* **273**, 1709–1714.

Lauritzen I., Chemin J., Honore E., Jodar M., Guy N., Lazdunski M. and Jane Patel A. (2005) Cross-talk between the mechano-gated K2P channel TREK-1 and the actin cytoskeleton. *EMBO Rep.* **6**, 642–648.

Lohmann C., Finski A. and Bonhoeffer T. (2005) Local calcium transients regulate the spontaneous motility of dendritic filopodia. *Nat. Neurosci.* **8**, 305–312.

Martinez-Quiles N., Rohatgi R., Anton I. M. *et al.* (2001) WIP regulates N-WASP-mediated actin polymerization and filopodium formation. *Nat. Cell Biol.* **3**, 484–491.

McCroskery S., Chaudhry A., Lin L. and Daniels M. P. (2006) Transmembrane agrin regulates filopodia in rat hippocampal neurons in culture. *Mol. Cell Neurosci.* **33**, 15–28.

Mejillano M. R., Kojima S., Applewhite D. A., Gertler F. B., Svitkina T. M. and Borisy G. G. (2004) Lamellipodial versus filopodial mode of the actin nanomachinery: pivotal role of the filament barbed end. *Cell* **118**, 363–373.

Ngo-Anh T. J., Bloodgood B. L., Lin M., Sabatini B. L., Maylie J. and Adelman J. P. (2005) SK channels and NMDA receptors form a Ca^{2+}-mediated feedback loop in dendritic spines. *Nat. Neurosci.* **8**, 642–649.

Ouyang Y., Wong M., Capani F. *et al.* (2005) Transient decrease in F-actin may be necessary for translocation of proteins into dendritic spines. *Eur. J. Neurosci.* **22**, 2995–3005.

Pedarzani P., Mosbacher J., Rivard A., Cingolani L. A., Oliver D., Stocker M., Adelman J. P. and Fakler B. (2001) Control of electrical activity in central neurons by modulating the gating of small conductance Ca^{2+}-activated K^+ channels. *J. Biol. Chem.* **276**, 9762–9769.

Pedersen K. A., Schroder R. L., Skaaning-Jensen B., Strobaek D., Olesen S. P. and Christophersen P. (1999) Activation of the human intermediate-conductance Ca(2+)-activated K(+) channel by 1-ethyl-2-benzimidazolinone is strongly Ca(2+)-dependent. *Biochim. Biophys. Acta* **1420**, 231–240.

Petrecca K., Miller D. M. and Shrier A. (2000) Localization and enhanced current density of the Kv4.2 potassium channel by interaction with the actin-binding protein filamin. *J. Neurosci.* **20**, 8736–8744.

Portera-Cailliau C., Pan D. T. and Yuste R. (2003) Activity-regulated dynamic behavior of early dendritic protrusions: evidence for different types of dendritic filopodia. *J. Neurosci.* **23**, 7129–7142.

Rimini R., Rimland J. M. and Terstappen G. C. (2000) Quantitative expression analysis of the small conductance calcium-activated potassium channels, SK1, SK2 and SK3, in human brain. *Brain Res. Mol. Brain. Res.* **85**, 218–220.

Rorth P. (2003) Communication by touch: role of cellular extensions in complex animals. *Cell* **112**, 595–598.

Schumacher M. A., Rivard A. F., Bachinger H. P. and Adelman J. P. (2001) Structure of the gating domain of a Ca^{2+}-activated K^+ channel complexed with Ca^{2+}/calmodulin. *Nature* **410**, 1120–1124.

Schwab A., Reinhardt J., Schneider S. W., Gassner B. and Schuricht B. (1999) K(+) channel-dependent migration of fibroblasts and human melanoma cells. *Cell Physiol. Biochem.* **9**, 126–132.

Small J. V., Stradal T., Vignal E. and Rottner K. (2002) The lamellipodium: where motility begins. *Trends Cell Biol.* **12**, 112–120.

Snapper S. B., Takeshima F., Anton I. *et al.* (2001) N-WASP deficiency reveals distinct pathways for cell surface projections and microbial actin-based motility. *Nat. Cell Biol.* **3**, 897–904.

Sousa A. D. and Cheney R. E. (2005) Myosin-X: a molecular motor at the cell's fingertips. *Trends Cell Biol.* **15**, 533–539.

Steffen A., Faix J., Resch G. P., Linkner J., Wehland J., Small J. V., Rottner K. and Stradal T. E. (2006) Filopodia formation in the absence of functional WAVE- and Arp2/3-complexes. *Mol. Biol. Cell* **17**, 2581–2591.

Stradal T., Courtney K. D., Rottner K., Hahne P., Small J. V. and Pendergast A. M. (2001) The Abl interactor proteins localize to sites of actin polymerization at the tips of lamellipodia and filopodia. *Curr. Biol.* **11**, 891–895.

Svitkina T. M., Bulanova E. A., Chaga O. Y., Vignjevic D. M., Kojima S., Vasiliev J. M. and Borisy G. G. (2003) Mechanism of filopodia initiation by reorganization of a dendritic network. *J. Cell Biol.* **160**, 409–421.

Tokuo H. and Ikebe M. (2004) Myosin X transports Mena/VASP to the tip of filopodia. *Biochem. Biophys. Res. Commun.* **319**, 214–220.

Wayman G. A., Kaech S., Grant W. F., Davare M., Impey S., Tokumitsu H., Nozaki N., Banker G. and Soderling T. R. (2004) Regulation of axonal extension and growth cone motility by calmodulin-dependent protein kinase I. *J. Neurosci.* **24**, 3786–3794.

Wittekindt O. H., Visan V., Tomita H., Imtiaz F., Gargus J. J., Lehmann-Horn F., Grissmer S. and Morris-Rosendahl D. J. (2004) An apamin- and scyllatoxin-insensitive isoform of the human SK3 channel. *Mol. Pharmacol.* **65**, 788–801.

Yoo Y., Wu X., Egile C., Li R. and Guan J. L. (2006) Interaction of N-WASP with hnRNPK and its role in filopodia formation and cell spreading. *J. Biol. Chem.* **281**, 15 352–15 360.

Zhang H., Berg J. S., Li Z., Wang Y., Lang P., Sousa A. D., Bhaskar A., Cheney R. E. and Stromblad S. (2004) Myosin-X provides a motor-based link between integrins and the cytoskeleton. *Nat. Cell Biol.* **6**, 523–531.

